



## EFFICIENT REMOVAL OF Pb<sup>2+</sup> ION FROM CONTAMINATED WATER UTILIZING SEAWEED POWDER AS AN BIOADSORBENT BASED ON PHYSICO-CHEMICAL INTERACTION

J. Michaelahitha Jose<sup>1</sup>, B. Vijila<sup>2</sup>, J. Joseph<sup>3,\*</sup>

### Abstract

Batteries, oil refining, dye production, lead mine drainage, and other sources are the principal sources of lead-containing waste water. The current research investigations were focused on the physico-chemical interaction with an adsorbent (made from Seaweed Powder (SP)) to remove Pb<sup>2+</sup> ions from waste water. SP adsorbent was prepared and examined using scanning electron microscopy, FT-IR, UV-visible. Through adjusting the pH, reaction duration, Pb<sup>2+</sup> concentration, and temperature, the adsorption property of SP was investigated. Systematic research has been done on selectivity, adsorption mechanisms, and reusability. The mass loss of SP at 333K, as determined by thermodynamic analysis. Our experimental findings from adsorption investigations revealed that temperature and adsorption efficiency were linearly related, while the initial metal level and adsorption effectiveness were inversely related. The observed experimental results indicated that the maximum temperature was 333K and the adsorption ability was 193 mg/g (94.87%). According to the equilibrium and thermodynamic findings, the Langmuir model ( $q_{\max} = 246.29 \text{ mg/g}$  and  $b = 0.79 \text{ L/mg}$ ) provided a more accurate description of the process. The adsorption procedure included both endothermic ( $\Delta H = 52.349 \text{ kJ/mol}$ ) and spontaneous ( $\Delta G = -24.104 \text{ kJ/mol}$ ) components. The electrostatic and chelation interactions between hydroxyl/amino groups and metal ions led to the optimized pH of 5. The adsorption behavior is well explained by Langmuir, and pseudosecond order kinetic models, demonstrating that the chemical reaction is the rate-limiting step and that the adsorption mechanism is monolayer adsorption. The adsorption was endothermic, impulsive, and practical, according to studies on thermodynamics. It is hoped that the developed SP will work well and last a long time to remove lead ions from wastewater.

**Keywords:** adsorbent, Seaweed, isotherm

<sup>1,2,3\*</sup>Dept. of Chemistry, Noorul Islam Centre for Higher Education, Kumaracoil-629180, Tamil Nadu, India e-mail id: joseph@niuniv.com

**\*Corresponding Author:** J. Joseph

\*Dept. of Chemistry, Noorul Islam Centre for Higher Education, Kumaracoil-629180, Tamil Nadu, India e-mail id: joseph@niuniv.com

**DOI:** 10.48047/ecb/2023.12.si10.00246

## **1. Introduction**

The globe is quite concerned about the quality of water. Natural or artificial contamination of water resources eventually has an impact on both human health and the economic and social growth of countries. Lead is one of the most hazardous chemical pollutants, and its deterioration in water quality has put billions of people's health at risk. Since UNICEF is a significant stakeholder in maintaining water quality through its activities around the world, clean drinking water becomes a crucial concern for UNICEF. The common global endeavour toward pollution remediation is the mitigation of contamination by efficient procedures.

Availability of fresh water for both human and industrial use is one of the socioeconomic difficulties we confront in the modern world. The declining amounts of this essential natural resource have also affected fauna and flora, particularly in Southern Africa [1]. In addition to many other issues, like increased climate change in small and medium-sized businesses, a lack of policies around childbirth, ongoing droughts, and overpopulation [2], Africa has been particularly affected by this issue. This is primarily caused by water and/or water body pollution, occasionally from polluted water. There are four types of pollutants in wastewater: pathogens, heavy metals and alkaline earth metals, organic and inorganic pollutants, and heavy metals [3,4].

Water body contamination from heavy metal and alkaline earth metal ions, primarily from chemical businesses, further exacerbates the issue of water scarcity. Heavy metal pollution has been exacerbated by chemical companies, including those that manufacture batteries, textiles, paints and dyes, tanneries, paint and dye manufacturing, and metal plating [5-8]. It has been established that alkaline earth and heavy metal ions, such as lead and zinc, are carcinogenic and can harm aquatic life and humans by causing cancer. This is due to its high toxicity, bio accumulative nature, and lack of biodegradability. Lead, arsenic, and chromium ions have been found in potable water and wastewater, which have been associated to lung cancer, kidney cancer, and other malignancies [9]. Along with being known to cause cancer, metals like lead and chromium have also been linked to teratogens and mutagens [1].

A massive amount of health problems, including mental instability, brain damage, retardation, and a reduction in haemoglobin synthesis, have been

linked to lead, which is also exceedingly poisonous. Because of all the difficulties listed above, governments and environmentalists have created tight procedures aimed at monitoring and lowering the amounts of heavy metal concentration in industrial effluents. The development of new and improved technologies that can manage heavy metals effectively and lower their concentration to below the established disposal limits has received a lot of research due to this strategy. Therefore, we are sure that the innovative component of our research is the ejection of Pb<sup>2+</sup> ions from wastewater by adsorption on surface modified bioadsorbent.

Due to separation and regeneration, the majority of proposed adsorbents haven't been financially viable; hence, research is still being done to determine the best adsorbent for removing heavy metal ions. Using natural composite adsorbents made of kaolinite and smectite, [10] studied the adsorption of Pb<sup>2+</sup> ions from wastewater. Positive results were discovered at pH 2, along with a linear relationship between adsorption rate and temperature from 30 to 75 °C, a linear relationship with adsorption capacity up to 100 mg/L, and an inverse relationship between adsorption and volume from 100 to 500 mg/L. Higher pH led to H<sup>+</sup> ions adsorbing instead of Pb<sup>2+</sup> ions. [11] used powdered *Albizia lebeck* pods as an adsorbent to study the adsorption of Pb<sup>2+</sup>, Zn<sup>2+</sup>, Cd<sup>2+</sup>, and Cu<sup>2+</sup> ions from aqueous solutions. They experimented with several settings and discovered that a pH 10, an agitation period of 30 minutes, a lesser earliest metal concentration of 10 mg/L, a immense adsorbent dosage of 1.4 g, and an elevated temperature (T) of 80 °C were the most effective. The Langmuir isotherm model (R<sub>2</sub> > 0.94), which describes the adsorption process the best. When the temperature was low, the process was endothermic and non-spontaneous; when the temperature was high, it was spontaneous.

There has been much research on the deletion of heavy metal ions from wastewater using surface modified adsorbents because it has been demonstrated that they have excellent properties like explicit pore size, high surface area, acceptable selectivity, and adsorption capacity. The adsorbent has different functional groups for effective removal of metal ions through Physico-Chemical interactions. These functional categories were used by several scholars, who made significant contributions to the expanding body of knowledge on this topic. The most important consideration when considering the removal of

metal ions from wastewater is a high capacity for adsorption, which is associated with a high surface area to volume ratio [12].

In this research, seaweed powder (SP) was used as an adsorbent to investigate the removal of Pb<sup>2+</sup> from aqueous solutions and wastewater samples. It is also explained how removal is influenced by other important factors like pH, adsorbent dosage, heavy metal concentrations, contact periods, and temperatures. Seaweed powder was discovered to have various advantages over other materials and to be an effective adsorbent for removing lead.

## 2. Experimental Details

### 2.1. Materials

Himedia provided all the chemicals and materials for our experimental work. We employed anhydrous potassium carbonate (AR, K<sub>2</sub>CO<sub>3</sub>, 99.9%), anhydrous hydrochloric acid (AR, HCl, 36%), deionized water (millipore), anhydrous sodium hydroxide (AR, NaOH, 99.9%), and anhydrous calcium chloride (AR, CaCl<sub>2</sub>.2H<sub>2</sub>O, 99%) to synthesise SP.

### 2.2. Methods

Additionally, the bioadsorbent was put through chemical characterization procedures for the examination of SP, including X-Ray diffraction (XRD), Scanning Electron Microscopy (SEM), FT-IR, and Thermogravimetric examination (TGA). In order to ascertain equilibrium data and adsorption thermodynamics, the current work largely focuses on the impact of temperature and initial metal ion concentration on the adsorption of Pb<sup>2+</sup> ions.

### 2.3. Preparation of SP

The seaweed was collected from sea, then crushed the seaweed using a pestle and mortar, then sieved with a 100-micron-scale screen. It was soaked in fresh water for an hour to remove the adhering pulp, washed thoroughly with the same tap water and then with double distilled water until reaching pH 7. For upcoming studies, the acquired fine powder was kept in an airtight container to guard against humidity [13].



Figure 1. Pictorial presentation of SP

### 2.4. Characterization techniques

The three main characterization methodologies used to evaluate the prepared adsorbent's intrinsic surface characteristics were surface morphology, thermal stability, and particle size (SP). These traits are frequently important for comprehending how heavy metals are ejected from aquatic environments. The outcomes from the SP's numerous analytical methods are summarised here.

#### 2.4.1. XRD analysis

The SP particles' XRD analysis is shown in Figure 4 with distinct peaks at 22.5°, 29.5°, 31.5°, 45°, 56.5°, and 75.5°, with a prominent peak at 22°. The particle size of the adsorbent, which was reflected in the adsorption of lead ions on its surface, is revealed by the power XRD spectrum.

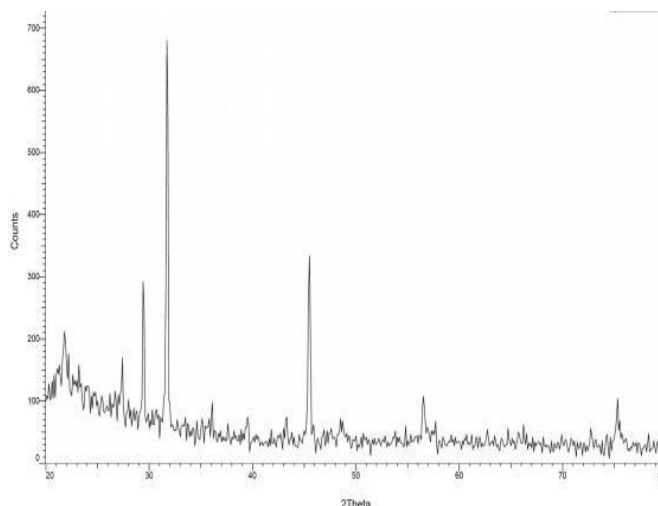


Figure 4. XRD pattern for SP particles.

### 2.4.2 FT-IR Spectrum of Adsorbent (SP)

The adsorbent (SP) exterior was examined to better understand the surface functional groups that were present, and its IR spectra were collected as shown in figure 2. Three strong bands were visible in the IR spectrum of SP (Fig.2) at 3340.6, 2980.2, and 1094.5  $cm^{-1}$ . Water chemisorbed on the surface and surface hydroxyl groups were blamed for the band at 3340.6  $cm^{-1}$ . The surface functional groups of SP are thought to play a role in the biosorption of  $Pb(II)$  from water. The sharp peak at 3450  $cm^{-1}$  can be explained by both the O-H stretching and the N-H stretching vibrations of amine groups. C-O and C=O were given to the absorption bands at 1094 and 1440  $cm^{-1}$ , respectively. Si-o-Si bonds were attributed to the peaks at 1120 and 840  $cm^{-1}$  in the fingerprint area. After  $Pb^{2+}$  sorption, the strength of the peaks at 1105 and 828  $cm^{-1}$  decreased, most likely due to the presence of absorption peaks for

other groups that are observable in the same spectral region. As a result of the C-O bond's altered electron density during  $Pb^{2+}$  biosorption, the peak at 1062  $cm^{-1}$  also exhibited an increase in intensity (II). The work of Singha and Das is supported by this (2012). The bands at 1604 and 1076.2  $cm^{-1}$  can be attributed to phosphate and silicate groups, respectively, and C=O stretching frequencies. The bands at 466.7 and 1438 and 1396  $cm^{-1}$  were caused by carboxylate groups. Lignin, lignocelluloses, and cellulose make up the SP's three primary parts. A strong band at 1041.5  $cm^{-1}$  demonstrates stretching of several C-OH and C-O-C bonds. It is clear from the IR spectrum that there are functional groups that can be ionised; their ionisation creates empty sites that metal ions can fill. This suggests that those substances might be utilised as adsorbent to remove heavy metals.

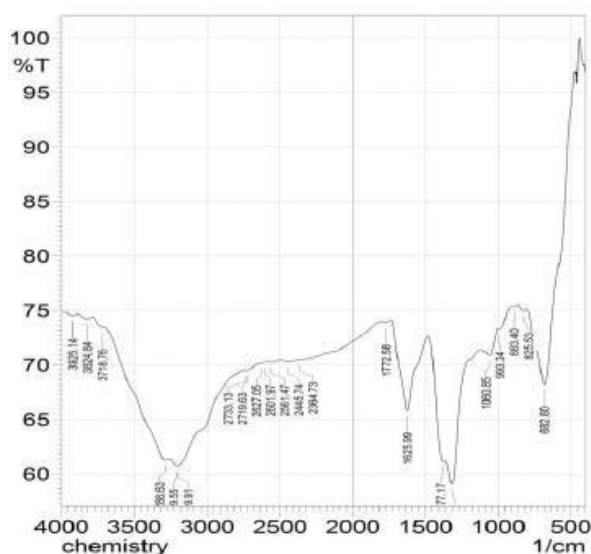


Figure 2. FT-IR spectrum of SP

### 2.4.3. Thermogravimetric analyses (TG/DTA)

A remarkably small material loss for TSP is seen in Figure 3. The entire material loss is estimated to be around 15% in this case. According to [14], the endothermic impact is thought to be caused by the loss of physically adsorbed moisture and appears to

extend up to 200 °C, but it appears to be a very low material loss of only 1% around 100 °C. According to the TG and DTA curves, additional endothermic effects are seen at temperatures of 655°C and at 815°C, respectively, with losses of about 3%.

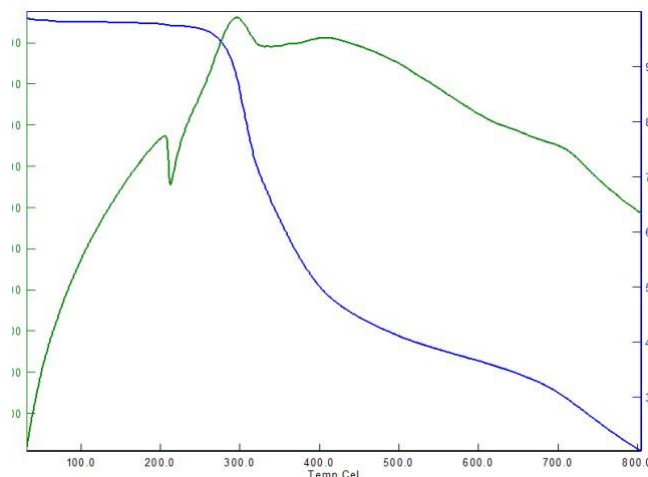


Figure 3. TG/DTA curves for SP particles.

### 2.4.4. SEM analysis

To learn crucial details about the nanoparticles' morphology, texture, size, and shape, we used SEM analysis. The micrographs of SP adsorbent are displayed in Figure 5. The particles in the picture are primarily spherical, and particle aggregation is also visible. The particles' size was determined to be between 100 and 200 nm. Additionally, it is difficult to distinguish individual particles from one another in the micrographs, making it difficult to determine the material's shape. The powder's visible, permeable microporous particles had distinct gaps between each molecule that serve as good metal ion binding sites. The separated biosorbent morphology can

absorb  $Pb^{2+}$  ions, as shown by the porosity and gaps between the activated seed coat biomass particles visible under SEM [15].

SEM images were used to analyse the chemical characteristics and adsorption mechanism of  $Pb^{2+}$  by adsorbent, SP. The irregular lamellar structure and honeycombed porous surface of the adsorbent are visible in images obtained using scanning electron microscopy (Fig. 5). The adsorbent is shown in Figs.5 (a&b) before and after  $Pb^{2+}$  ion adsorption. It can be noticed that the adsorbent surfaces have some oval material on them, which suggests that  $Pb^{2+}$  ion adsorption has altered the adsorbent surface.

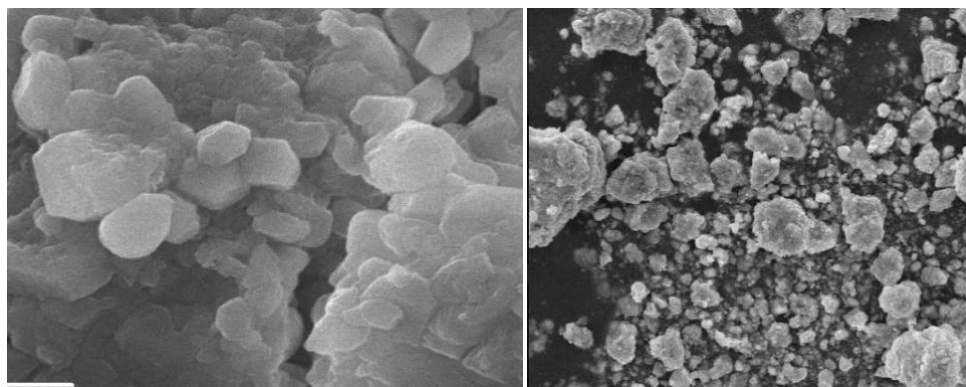


Figure 5. (a) SEM images of adsorbent alone (b) SEM micrograph of adsorbent react with  $Pb^{2+}$  ions.

## 3. Results and discussion

### 3.1. Adsorption studies

We looked at SP's ability to remove  $Pb^{2+}$  ions. Temperature and initial sorbate concentration were

two of the many adsorption parameters that we extensively examined.

### 3.1.1. Effect of pH

$Pb^{2+}$  ions adsorption is significantly influenced by the pH of an aqueous solution. It establishes the surface characteristics of the adsorbent in terms of surface charges, functional group ionization, and level of functional group dissociation at active sites [16]. The highest  $Pb^{2+}$  adsorption occurred at 90% for SP adsorbent at an optimum pH of 5. When the pH of the contaminated water increases from 1-5,

$Pb^{2+}$  is more readily absorbed. This may be due to the growth of  $Pb^{2+}$  and decreased competition between metal ions and hydroxonium ions ( $H_3O^+$ ) in waste water. The optimal pH for the majority of metal adsorption by a variety of adsorbents has been reported in numerous adsorption studies to be in the range of 4-6. This might be caused by the solution containing an excessive amount of  $OH^-$  ions.

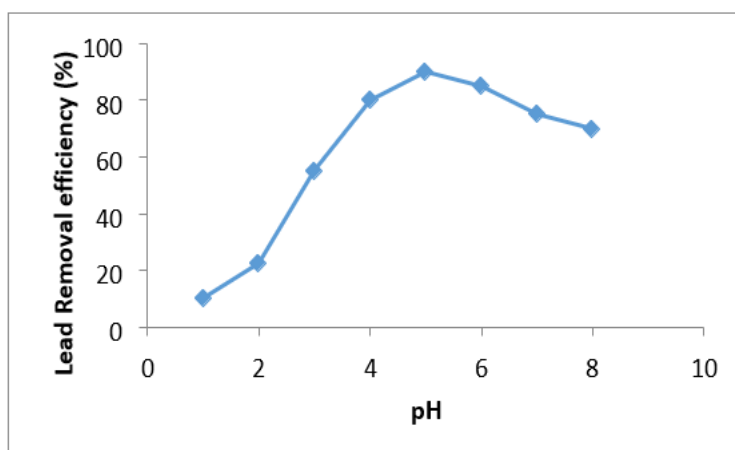


Figure 6. Effect of pH on SP

### 3.1.2. Effect of Adsorbent Dosage

The effect of the SP dose on  $Pb^{2+}$  is shown in Figure 7. Due to the increasing availability of adsorbent,

the  $Pb^{2+}$  uptake rate raise as gives maximal removal efficiency 85% at 50mg/L.

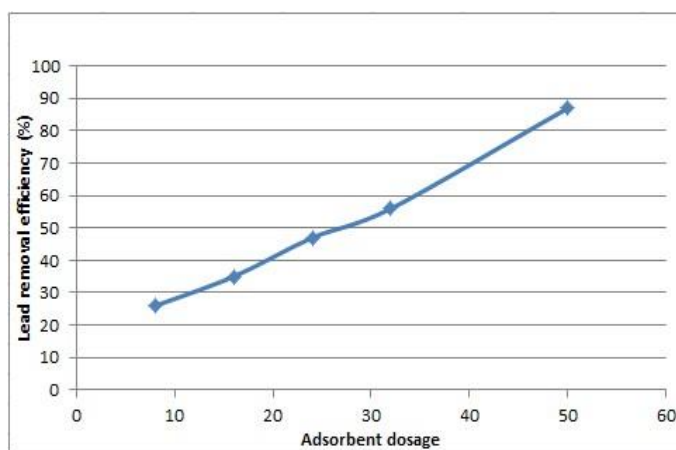


Figure 7. Effect of Adsorbent Dosage of SP

### 3.1.3 Effect of contact time

For SP,  $Pb^{2+}$  removal efficiencies relative to contact time with different adsorbent dosages of 10, 20mg/L are shown in Figure 8. By observing the uptake of the  $Pb^{2+}$  ions over a period of 70 min at room temperature, the impact of contact duration was ascertained. Within 70 minutes, the elimination of  $Pb^{2+}$  as a percentage reached its peak (87%). The presence of free active sites at the adsorbent surfaces, which gradually became

occupied by  $Pb^{2+}$  ions over the course of the next 70 minutes, may have contributed to the removal efficiency that occurred so quickly in the beginning. Because  $Pb^{2+}$  ions [17,18] competed for fewer active sites as the binding sites became exhausted, the uptake rate dropped. A decrease in the boundary layer resistance to mass transfer around the sorbent particles was another factor contributing to the improvement in removal efficiency during longer contact times.

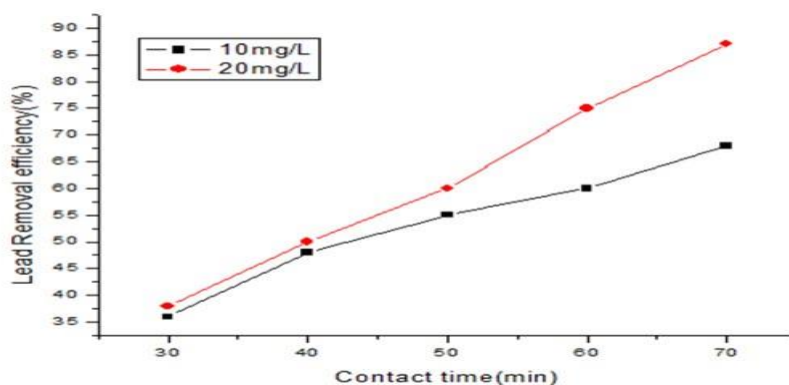


Figure 8. Effect of Contact Time on SP

### 3.1.4 Effect of Stirring rate

The effect of varying the stirring rate on the  $Pb^{2+}$  removal efficiency of SP is shown in Figures 9. It shows that increasing the stirring rate from 20

to 120 rpm increases the percentage adsorption, with SP reaching a limit of 82.5% adsorption at around 120 rpm.

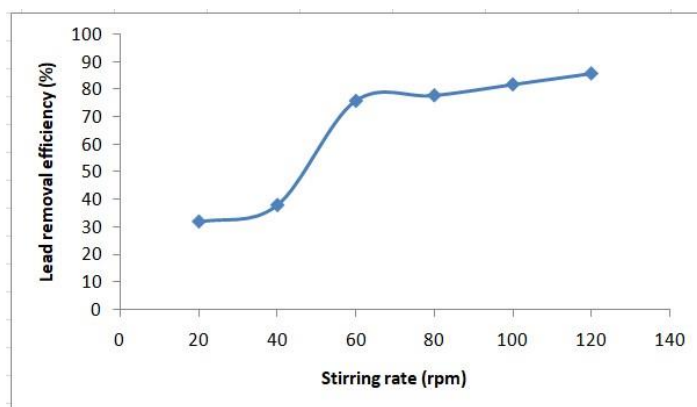


Figure 9. Effect of stirring Rate on SP

### 3.1.5 Effect of Temperature

According to Figure 10, increasing the temperature from 280 to 330 K raises both the percentage of

$Pb^{2+}$  adsorption and the adsorption ability. The removal efficiencies of adsorbent SP (94%) increased with increasing temperature (330K).

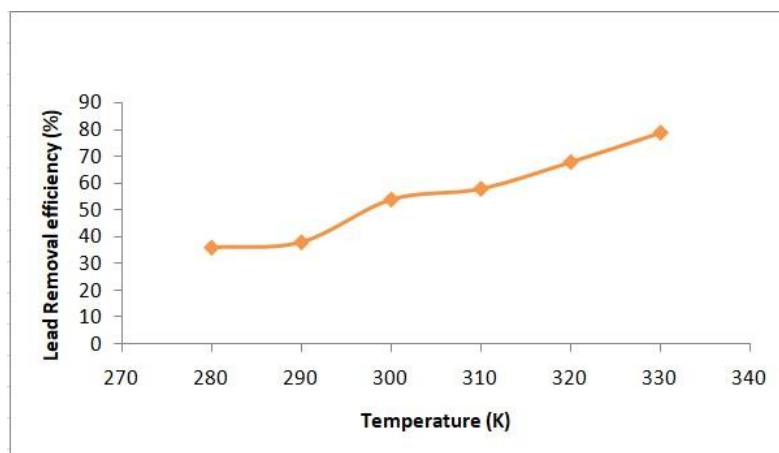


Figure 10. Effect of Temperature on SP

### 3.2 Thermodynamic Study

The thermodynamic parameters were determined using  $\log (q_e/C_e)$  vs  $1/T$  in order to evaluate the thermodynamic probability as well as the

spontaneity of the adsorption process. The endothermic and spontaneous nature of the adsorption is suggested by the positive  $\Delta H^\circ$  and  $\Delta G^\circ$ . The  $\Delta G^\circ$  decreases as temperature rises from

313 to 333 K, showing that the reaction is more favourable as temperature rises, which is consistent with the nature of entropically advantageous exothermic reactions. The thermodynamic findings agree with the kinetic studies' findings of an increase in adsorption density and lead removal effectiveness. The thermodynamic link suggested by [19] between  $\Delta G^\circ$ ,  $\Delta S^\circ$ , and  $\Delta H^\circ$ . The temperature rises from 313 to 333 K, while the  $\Delta G^\circ$  value is -24.104 kJ/mol. The fact that the  $\Delta G^\circ$  value lowers as the temperature rises indicates that the lead sorption capacity of SP improves with temperature. If  $\Delta G^\circ$  is negative, adsorption is both possible and spontaneous. The overall endothermic nature of the sorption process is shown by the positive  $\Delta H^\circ$  value, 52.349 kJ/mol.  $\Delta S^\circ$  is estimated to be between 1.36 and 1.38 kJ/mol K. A good  $\Delta S^\circ$  value suggests that SP has a strong affinity for  $Pb^{2+}$  and could also mean that the level of disorder is rising.

Positive  $\Delta S^\circ$  values suggest that lead adsorption happens on its own.

### 3.3 Regeneration study

Adsorbent reusability is the focus of regeneration experiments, which save money and reduce

pollution. Traditional acids and bases are utilised in this regeneration study. HCl or NaOH were used to test the adsorbent's ability to regenerate. During the action, HCl can induce metal component leakage and adsorbent damage, whereas NaOH promotes  $Pb^{2+}$  replacement and has been found to be the most efficient solution for adsorbent renewal. Batch experiments were used to test the SP adsorbents. Because a larger NaOH concentration can alter the configuration of adsorbents, a lower NaOH concentration was used for this adsorbent regeneration method. The adsorbent was taken at a concentration of 35 mg/L and mixed with NaOH for 180 mins. The adsorbent was filtered and dried for four hours at 97°C. In similar conditions, the recycled adsorbent was employed again. The SP removal efficiency was 72% in the 5<sup>th</sup> cycle. The removal efficiency was reduced due to a lack of adsorbent active sites. When regenerated adsorbents were particularly in comparison to other adsorbents in the literature, adsorbents were found to have a higher reusability. Adsorbents can be used again due to their microporous arrangement and larger surface area, lowering the overall cost of the adsorption process in practical applications.

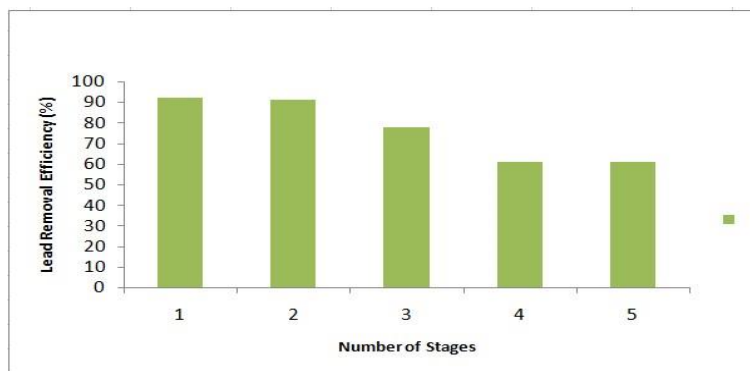


Figure 11. Plot of  $Pb^{2+}$  Removal Efficiency Vs Number of stages for SP

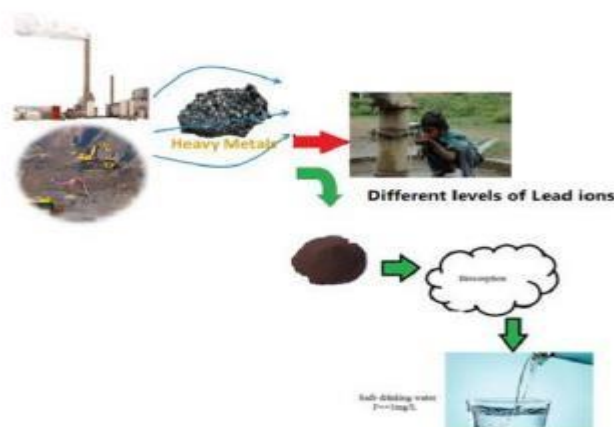


Figure 12. Schematic representation of  $Pb^{2+}$  contaminated water into drinking water



### 3.4 Adsorption Isotherm studies

Figure 13 depicts lead adsorption on SP by showing the graph against  $1/C_e$  vs  $1/q_e$  in the Langmuir model, which yields a straight line and slope. The Langmuir constants  $R^2$ ,  $K_L$ , and  $q_m$  were calculated using the intercept and slope graphs. The intercept and slope values for the Freundlich model were calculated using the graph ( $\log C_e$  vs  $\log q_e$ )

displayed in figure 14. The correlation values of 0.9979, 0.9922 and 0.8272 were obtained from Langmuir, Freundlich and Temkin models. The greater  $R^2$  value of the Langmuir model compared to other isotherms indicated that Langmuir was the best fit and confirmed that the adsorbent surface was homogeneous.

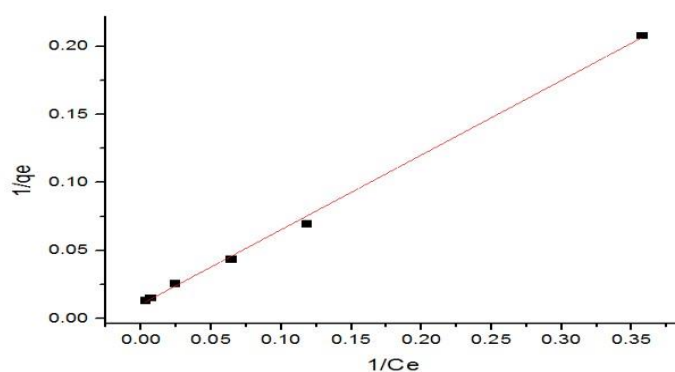


Figure 13. Langmuir model for SP

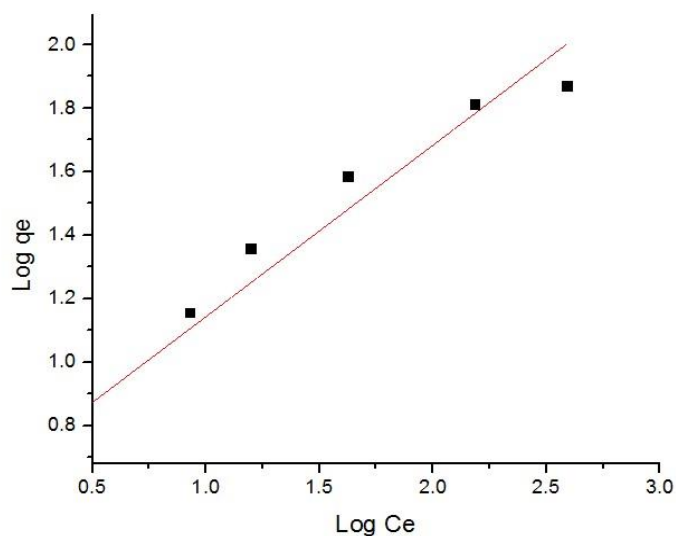


Figure 14 : Freundlich model for SP

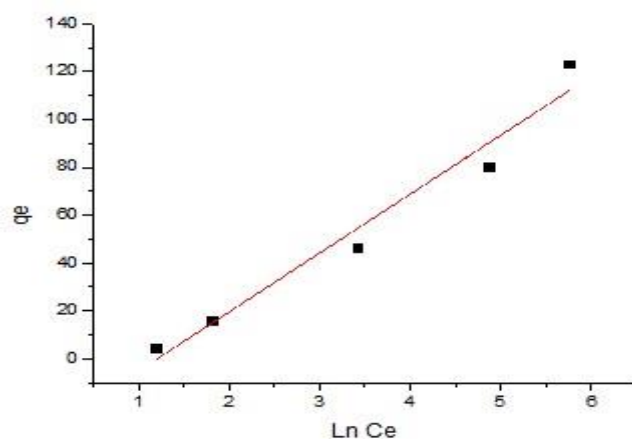


Figure 15: Temkin model for SP

The correlation values of 0.99797, 0.9922, and 0.8272 were obtained using the Langmuir, Freundlich, and Temkin models. The greater  $R^2$  value of the Langmuir model compared to other isotherms indicated that Langmuir was the best fit and confirmed that the adsorbent surface was homogeneous.

The results showed that the SP was not the right match for PFO since the practical and theoretical

data did not match up properly, according to the PFO kinetic study of SP on Pb adsorption (Figure 16). In this instance, PSO was used to match the data (Figure 17). The slope and intercept for the graph of  $t$  vs  $t/q_t$  are  $q_e$  and  $K_2$ , respectively. The pseudo second order model suited the data better than the pseudo first order model, where the  $R^2$  was 0.9986, which was closer to 1.

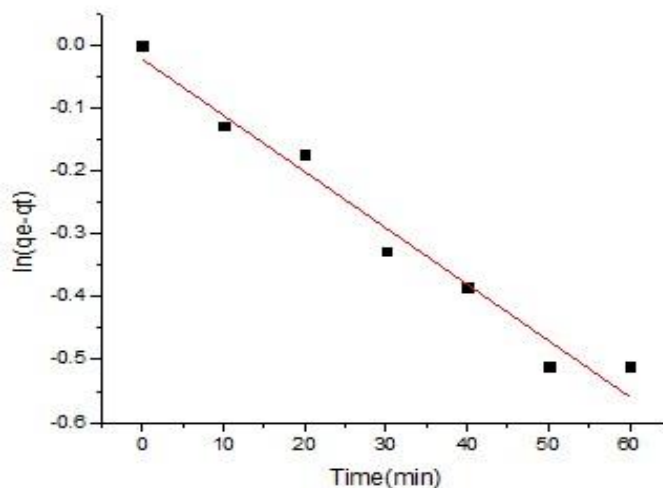


Figure 16: PFO kinetics for SP

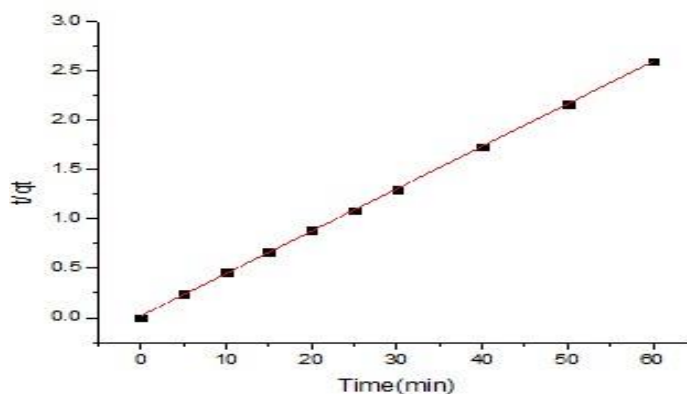


Figure 17: PSO kinetics for SP

## Conclusion

With the use of the characterization procedures, we were able to successfully prepare SP (adsorbent), which was then confirmed. The  $Pb^{2+}$  ions were subsequently taken out of the wastewater using the SP adsorbent. Our experimental findings lead us to the conclusion that  $Pb^{2+}$  ion adsorption onto SP is influenced by temperature and the initial metal ion concentration. We showed that the equilibrium sorbate concentration and adsorption capacity are best explained by the Langmuir model, indicating that monolayer adsorption took place. We also deduced that the ideal  $Pb^{2+}$  ion adsorption capacity of SP was 193 mg/g. According to the results of our

investigation, waste water's  $Pb^{2+}$  ions adsorb in a monolayer on the adsorbent surface. As a result of our findings, we came to the conclusion that the removal of the  $Pb^{2+}$  ion by SP is an endothermic adsorption process as indicated by the positive value of the thermodynamic parameter. The negative  $\Delta G^\circ$  indicates that the adsorption is spontaneous.

We'd like to summarise our findings by saying that the SP has effective adsorption properties for  $Pb^{2+}$  ions from contaminated water, and we draw the conclusion that SP can be employed for  $Pb^{2+}$  ion removal in industrial settings. In the future, it will

be necessary to test SP to see if it can remove heavy metals like arsenic and chromium. Since the adsorption procedure in this current study was batch-wise, a more thorough investigation employing a continuous system is strongly advised. This is due to the fact that continuous systems more closely resemble the industrial configuration. The cost of the adsorbent should also be reduced by conducting desorption and reusability test trials because it will be more appealing if it can be used repeatedly.

## References

1. U.F.C. Sayago, Y.P. Castro, L.R.C Rivera, A.G. Mariaca, Estimation of equilibrium times and maximum capacity of adsorption of heavy metals by *E. crassipes* (review), *Environ. Monit. Assess.*, 192(2020), p.141.
2. S. Singh, K.C. Barick, D. Bahadur, Functional Oxide nanomaterials and nanocomposites for the removal of heavy metals and dyes, *Nanomater. Nanotechnol.* (2013), pp. 3-20
3. S.H. Huang, D.H. Chen, Rapid removal of heavy metal cations and anions from aqueous solutions by an amino-functionalized magnetic nano-adsorbent, *J. Hazard. Mater.*, 163 (2009), pp. 174-179
4. S. Singh, K.C. Barick, D. Bahadur, Surface engineered magnetic nanoparticles for removal of toxic metal ions and bacterial pathogens, *J. Hazard Mater.*, 192 (2011), pp. 1539-1547
5. A.Z.Md. Badruddoza, Z.B.Z. Shawon, Md.T. Rahman, K.W. Hao, K. Hidajat, M.S. Uddin, Ionically modified magnetic nanomaterials for Arsenic and Chromium removal from water, *Chem. Eng. J.*, 225 (2013), pp. 607-615
6. Hao, Y. Zhong, F. Pepe, W. Zhu, Adsorption of Pb<sup>2+</sup> and Cu<sup>2+</sup> on anionic surfactant templated amino-functionalized mesoporous silica, *Chem. Eng. J.*, 189-190 (2012), pp. 160167
7. Mohammadifard, M.C. Amiri, Evaluating Cu(II) removal from aqueous solutions with response surface methodology by using novel synthesized CaCO<sub>3</sub> nanoparticles prepared in a colloidal gas aphon system, *Chem. Eng. Commun.*, 204 (4) (2017), pp. 476-484
8. R. Gusain, N. Kumar, E. Fosso-Kankeu, S.S. Ray, Efficient removal of Pb(II) and Cd(II) from industrial mine water by a hierarchical MoS<sub>2</sub>/SH-MWCNT nanocomposite, *ACS Omega*, 4 (2019), pp. 13922-13935
9. K. Li, L. Xie, Z. Hao, M. Xiao, Effective removal of Hg(II) ion from aqueous solutions by thiol functionalized cobalt ferrite magnetic mesoporous silica composite, *J. Dispersion Sci. Technol.*, 41 (4) (2020), pp. 503-509
10. I.M. El-Naggar, S.A. Ahmed, N. Shehata, E.S. Sheneshen, M. Fathy, A. Shehata, A novel approach for the removal of lead (II) ion from wastewater using Kaolinite/Smectite natural composite adsorbent, *Appl. Water Sc.*, 9 (2019), p. 7.
11. S. Mustapha, D.T. Shuaib, M.M. Ndamitso, M.B. Etsuyankpa, A. Sumaila, U.M. Mohammed, M.B. Nasirudeen, Adsorption isotherm, kinetic and thermodynamic studies for the removal of Pb(II), Cd(II), Zn(II) and Cu(II) ions from aqueous solutions using *Albizia lebbek* pods, *Appl. Water Sci.*, 9 (2019), p. 142
12. T. Kegl, A. Košak, A. Lobnik, Z. Novaka, A. Kovač Kralj, I. Ban, Adsorption of rare earth metals from wastewater by nanomaterials: a review, *J. Hazard Mater.*, 386 (2020).
13. Zhang, W., Mao, S., Chen, H., Huang, L., Qiu, R., 2013. Pb(II) and Cr(VI) sorption by biochars pyrolyzed from the municipal wastewater sludge under different heating conditions. *Bioresour. Technol.* 147, 545-552.
14. A. Mourhly, M. Khachani, A. El Hamidi, M. Kacimi, M. Halim, S. Arsalane, The synthesis and characterization of low-cost mesoporous silica SiO<sub>2</sub> from local pumice rock, *Nanomater. Nanotechnol.*, 5 (2015), p. 35
15. Aju Mathew George, Ajay R. Tembhurkar, "Analysis of equilibrium, Kinetic, and thermodynamic parameters for biosorption of fluoride from water onto coconut (*Cocos nucifera* Linn.) root developed adsorbent, *Chinese Journal of Chemical Engineering* 27(2019) 92-99.
16. Mondal Poonam, George Suja and Mehta Dhiraj, "Use of calcite for defluoridation of Drinking water in Acidic medium, *Research Journal of Chemical Sciences*, 4(6),62-65, June (2014).
17. Alaa Kareem Mohammed, Safaa Abdalrasool Ali, Ali Muayyed Najem, Kais Kassim Ghaima, Effect of Some Factors on Biosorption of Lead by Dried Leaves of Water Hyacinth (*Eichhornia Crassipes*), *Int. J. Pure Appl. Sci. Technol.* 17 (2013)72-78.
18. F. Chigondo, B.C. Nyamunda, S.C. Sithole, L. Gwatidzo, Removal of lead (II) and copper (II) ions from aqueous solution by baobab (*Adononia digitata*) fruit shells biomass, *J. Appl. Chem.* 5 (2013) 43-50.
19. V.K. Gupta, A. Rastogi, "Biosorption of lead from aqueous solutions by green algae *Spirogyra* species: Kinetics and equilibrium studies", *Journal of Hazardous Materials*, 152, (2008), 407-414.